Initial results for comparing three approaches to set TACs for the major fisheries in the SIOFA area of the Southern Indian Ocean

Anabela Brandão, Doug S. Butterworth and Susan Johnston

Marine Resource Assessment and Management Group (MARAM)
Department of Mathematics and Applied Mathematics
University of Cape Town, Rondebosch, 7701, South Africa
January 2022

ABSTRACT

Simulation studies are used to provide a generic comparison of three approaches to set TACs for a selected stock of each of alfonsino, orange roughy and toothfish in the SIOFA region. These are reduction in the TAC only if there is a high probability of a recent downward trend in the abundance index (APR1), a TAC that fluctuates up or down proportional to recent changes in that index (APR2), and a fitted population model-harvest control rule combination (APR3). To achieve sensible target depletions after 20 years, case-specific selections of initial upward or downward trends in TACs are found to be needed. For technical reasons, the toothfish stock selected proves an unsatisfactory choice for this exercise. Furthermore, results for the orange roughy stock are dominated by the need to reduce current catches substantially to achieve sustainability, rendering comparisons of the approaches problematic. For alfonsino, APR1 is preferred to APR2 because of future TACs show smoother trends in the future; however, consideration of APR3 would need further robustness tests to be investigated to offset its current advantage of equivalence between the testing model and the population model fitted within the procedure. It seems, however, that certain control parameter value choices (especially the size of the initial trend in the TAC) are likely to need to vary substantially from stock to stock, requiring stock-specific as well as generic analyses to proceed further with this investigation. Consequently, the prospects for developing entirely generic approaches/harvest strategies able to cover the major resources in the SIOFA region do not appear promising. A roadmap with suggestions about how SIOFA might best move forward towards adopting such harvest strategies in these circumstances will be put forward as the second part of this project.

KEYWORDS: Harvest strategies, Southern Indian Ocean, Alfonsino, Orange roughy, toothfish, simulation, TAC

INTRODUCTION

This document presents initial results of a generic investigation of alternative approaches (harvest strategies) to set TACs for the major SIOFA resources, to provide a basis to choose between them. Here the analyses are based on sub-components of the alfonsino and of the orange roughy resources. This investigation is pursued NOT to provide an optimal proposal for those stocks, but rather to use them as typical examples of the major resources in the SIOFA region and the data available for them.

DATA

Alfonsino

The annual total catches of alfonsino for the West area of the SIOFA area of the Southern Indian Ocean and the relative abundance indices for "fleet" S2 (for the West area) obtained from CPUE standardisation as reported in Brandão and Butterworth (2020) are used to investigate the approaches for computing future TACs. Table 1 shows the catch (removals) figures summed over the three fleets for which CPUE data are available, as well as catches from other member and non-member countries. These catch data, as reported in Brandão and Butterworth (2020), are available for the period from 1977 to 2018. Given the non-availability of data since 2018, it has been assumed that the catches for 2019 and 2020 are the same as that for 2018. As TACs are not set at present for alfonsino, a TAC for 2021 equal to the (rounded) catch in 2020 is assumed, together with the assumption that it is fully taken by the fishery. (Note that the accuracy of these assumptions is not critical here, given the generic nature of this investigation.)

The standardised CPUE indices reported in Brandão and Butterworth (2020) for the S2 "fleet" are also listed in Table 1. Future CPUE indices are generated commencing from 2019.

Orange Roughy

The annual total catches of orange roughy for Feature 4 of the SIOFA area of the Southern Indian Ocean, and the associated abundance indices obtained from acoustic surveys, are used to investigate the different approaches for computing future TACs. Table 1 shows the catch (removals) as reported in Cordue (2018), which are available for the period from 2001 to 2017. Given the non-availability of data since 2017, it has been assumed that the catches for the period 2018 to 2020 are the same as that for 2017. As TACs are not set at present for orange roughy, a TAC for 2021 equal to the (rounded) catch in 2020 is assumed, together with the assumption that it is fully taken by the fishery.

The acoustic biomass estimates and the corresponding CVs reported in Cordue (2018) and Macaulay (2021) for Feature 4 are also listed in Table 1. Future survey indices are generated assuming that an acoustic survey will take place every five years commencing from 2023.

OPERATING MODELS AND PROJECTIONS

Alfosino

The results of Brandão and Butterworth (2020) included the conditioning of a Reference Set (RS) of Operating Models (OMs) to be used to generate future data to test different approaches (APRs) for setting TACs. Here the Base Case OM is used. The methodology for the generation of future data is given in Appendix A. The biological parameter values as well as OM parameter values necessary for this generation are listed in Table 2.

Orange roughy

An Age-Structured Production model (ASPM) has been applied to orange roughy data to condition an OM to be used to generate future data. The ASPM incorporates the historical catches, the acoustic abundance indices (together with their CVs) as listed in Table 1, as well as the biological parameter values assumed (Table 2). The ASPM for orange roughy is similar to that applied to the alfonsino resource, except that for orange roughy the abundance indices are assumed to be absolute with a value of proportionality (q) of 0.8. In the absence of catch-at-length data, the selectivity curve could

not be estimated and was assumed to be knife edge as in Cordue (2018). Appendix A details the methodology for generating future orange roughy data.

THE APPROACHES CONSIDERED

Alfonsino

APR1

APR1, where catches (TAC) are maintained at present levels, unless there is evidence of a marked downward trend in resource abundance indices (such as CPUE or survey abundance indices), is specified as

$$\text{APR1:} \quad TAC_{y+1} = \begin{cases} (1+\theta)TAC_y & \text{until first time TAC decreases} \\ TAC_y[1-\lambda] & \text{if } s_y^{LCI} < -\delta \\ TAC_y & \text{otherwise} \end{cases}, \qquad (1)$$

where s_y^{LCI} is the lower $100(1-\alpha)^{\text{th}}$ confidence interval value $\left(s_y - z_{\alpha/2} se_{s_y}\right)$ of the slope $\left(s_y\right)$ of a log-linear regression of the abundance CPUE indices (for the S2 "fleet" for alfonsino) against time for the years $y-10$ to $y-1$, θ determines the percentage by which the TAC is increased until the first time the APR rule results in a decrease in TAC and λ and δ are control parameters. The control parameter λ denotes the proportion by which the TAC is decreased, while δ is the value of the downward trend beyond which the TAC will be modified.

Initial investigation led to the selection of control parameters of $\delta = 0.18$, the lower bound of a 95$^{\text{th}}$ confidence interval ($\alpha = 0.05$), $\lambda = 0.05$ and $\theta = 4\%$. The results shown in Appendix B are for different values of the control parameter θ (2%, 3% and 4%). Note that these selections were made aiming to get similar minimum lower 5%-iles for spawning biomass projections over the 20-year projection period considered.

APR2

APR2, where the TAC varies in proportion to the results from continued collection of some measure or index of resource abundance (such as CPUE or survey abundance indices) is specified as

$$\text{APR2:} \quad TAC_{y+1} = (1+\theta)\overline{C_y}\left(\frac{\overline{CPUE}_{\text{current}}}{\mu_y^{CPUE}}\right), \qquad (2)$$

where θ determines the percentage by which the TAC is increased, μ_y^{CPUE} is the mean CPUE (for the S2 "fleet" for alfonsino) for the last three years for which there are historical data (i.e., here for 2016, 2017 and 2018), $\overline{C_y}$ is the mean annual catch for those same three years and $\overline{CPUE}_{\text{current}}$ is the mean current CPUE index for the years $y-2, y-1$ and y of the S2 "fleet" in the case of alfonsino.

In addition, this APR constrains TACs to a maximum inter-annual change of $x\%$. There are no control parameters in this approach to which to tune, but results are shown in Appendix B for various values (20% and 50%) of the maximum inter-annual increase change in TAC allowed, and for a value of 5% for the maximum decrease change in TAC. These options result in similar minimum lower 5%-iles for spawning biomass projections over the 20-year projection period to those for APR1. A value of 50% of the maximum inter-annual increase change in TAC allowed has been selected as the preferred value.

APR3

With APR3 the TAC is based primarily on some multiple of a proxy value of F_{MSY}, where this in turn is based on a proxy value for a B_{MSY} reference point whose value is informed by the most recent assessment of the resource. The specification is

$$\text{APR3:} \quad TAC_{y+1} = \begin{cases} (1+\theta)\Psi & \text{if } y \leq 2026 \\ \Psi & \text{otherwise} \end{cases}, \tag{3}$$

where θ determines the percentage by which the TAC is increased and Ψ is given by

$$\Psi = \begin{cases} \omega\tau\hat{F}^{*}_{MSY}\hat{B}^{sp}_{y} & \text{if } \hat{B}^{sp}_{y} < 1.2\hat{B}^{sp}_{MSY} \\ \omega\tau\hat{F}^{*}_{MSY}\left(1.2\hat{B}^{sp}_{MSY}\right) & \text{otherwise} \end{cases}, \tag{4}$$

where ω is a control parameter, $\hat{F}^{*}_{MSY} = \frac{M\hat{S}Y}{\hat{B}^{sp}_{MSY}}$ is a proxy for F_{MSY} and is estimated given the most recent assessment of the resource, $\hat{B}^{sp}_{y}$ is the most recent estimated spawning biomass and τ is given by

$$\tau = \begin{cases} 1 & \text{if } B^{sp}_{y}/K^{sp} > 0.4 \\ \vartheta & \text{if } 0.2 < B^{sp}_{y}/K^{sp} < 0.4, \\ 0 & \text{if } B^{sp}_{y}/K^{sp} < 0.2 \end{cases} \tag{5}$$

where ϑ indicates a linear increase from 0 to 1 as B^{sp}_{y}/K^{sp} increases from 0.2 to 0.4.

This APR also constrains TACs to a maximum inter-annual change of $x\%$. A value of 0.6 for the ω control parameter has been selected, together with a 20% maximum inter-annual increase change and a 5% maximum decrease change in TAC allowed. Appendix B shows results for different values of the control parameter ω.

Orange roughy

In broad terms, the APR's here are of the same general form as APR1, APR2 and APR3 (though the last has not yet been attempted). However, the different rate of acquisition of new data (one year every five instead of every year as with the alfonsino APR's necessitates some changes at a detailed level, which are set out below.

APR1

This approach for orange roughy is same as APR1 for alfonsino, except that acoustic survey abundance indices replace CPUE indices and all available survey indices are used to calculate the trend.

Using similar criteria as for alfonsino led to the selection of control parameters of $\delta = 0.05$, the lower bound of a 95th confidence interval ($\alpha = 0.05$), $\lambda = 0.1$ and $\theta = 4\%$ (though this does not come into play in this example, as the TAC decreases immediately for other reasons). The results shown in Appendix C are for a different value of the control parameter λ (0.15).

APR2

APR2 is given by the same form as APR2 for alfonsino, with the CPUE abundance statistics replaced with acoustic survey abundance statistics slightly adjusted to account for the infrequency of surveys. In this case, μ_{y}^{Survey} is the mean acoustic survey abundance for all years for which there are historical

data (i.e., here for 2007, 2009 and 2018), $\overline{C_y}$ is the mean annual catch for the last three years for which there are historical data (i.e., here for 2015, 2016 and 2017) and $\overline{Survey}_{\text{current}}$ is the mean current survey index for the last three survey indices available.

This APR also constrains TACs to a maximum inter-annual change of $x\%$. Results are shown in Appendix C for various values (10% and 50%) of the maximum inter-annual increase or decrease change in TAC allowed. A value of 10% of the maximum inter-annual increase or decrease change in TAC allowed has been selected as the preferred value.

RESULTS AND DISCUSSION

Alfonsino

Results for different choices for the values of the control parameters for APR1, APR2 and APR3 are shown in Appendix B. Figures 1 and 2 below consider single cases for each of these, selected to be roughly comparable is terms of the lower 5%-iles for spawning biomass projections over the 20-year projection period considered.

In a strategic context, given that these choices were made to achieve similar levels of resource depletion, the main basis for choice between the two approaches lies with future performance in terms of catch, i.e., the first row of panels in each of Figures 1 and 2. There, when compared to APR2, APR1 shows both a lesser range of future catches (Figure 1), plus much smoother catch trajectories for individual projection realisations (Figure 2). Hence APR1 would clearly seem to be the preferred of these two options.

Viewed in that light, the results in Figure 1 for APR3 seems certainly better still than those for APR1, with little to choose between the two in Figure 2. However, there is a "problem" with this comparison, as APR3 has an "unfair" advantage in this particular comparison – the population model used for estimation in APR3 is identical to that of the underlying OM, whereas in reality those two could well be rather different. Figures 3 and 4 give initial insight into the implications of that difference – there the population model used for APR3 can assume higher or lower values of steepness *h* than the 0.75 of the OM, and the corresponding catches and final spawning biomass depletions become very different.

Basically, the use of a population model in APR3 requires first fuller robustness checking, not only by considering OMs with different values of steepness *h* than 0.75 (APR1 and APR2 would also need to be tested for robustness to this); but more importantly APR3 would need to be extended to try to incorporate better feedback control by estimating *h* as well as K^{sp} in its model fitting process. That, however, will probably introduce considerably more variation into the estimates of these two model parameters, and hence in TACs output from year-to-year. That in turn could well negate the apparent advantages shown for APR3 over APR1 in Figures 1 and 2.

Orange roughy

Figures 5 and 6 show results for orange roughy that correspond to Figures 1 and 2 for alfonsino. However, with a new abundance estimate from surveys only once every five years, there is really insufficient contrast between the results for APR1 and APR2 to make any strategic choice.

This is partly a result of the fact that recent catches from this resource are unsustainable, so that the immediate priority is for these to be reduced – the aspect then dominates other features of the results. Given that, there seemed no immediate priority to pursue these calculations for APR3 for orange roughy.

Results for different values of the control parameters for APR1 and APR2 are shown in Appendix C.

Toothfish

The analyses pursued for alfonsino and orange roughy could not be duplicated for toothfish. The reason arises from the nature of the catch and CPUE trends for the toothfish stock put forward. Presently, there has only been a preliminary analysis of the toothfish resource in the Del Cano Rise which falls within the SIOFA area (Sarralde *et al.,* 2020). This stock is in its initial stages of harvesting, yet it reflects concurrent increasing trends in both catch and CPUE. This is not compatible with standard population dynamics assumptions and/or CPUE being proportional to abundance. Hence there was no basis to develop an OM to provide the basis to simulation test different APRs.

OVERVIEW

The combination of nature of the statuses of the three stocks investigated here, and the limited data available for them, leads to limitations in what can be achieved in terms of the original objectives for this work:

- The Operating Models required for testing cannot be (straightforwardly) developed for the toothfish stock.
- Results for the orange roughy stock are dominated by the need to reduce current catches substantially to achieve sustainability.
- For alfonsino, more work on robustness tests would be needed before initial comments could be made by way of a comparison between the performance of the population model-based APR3 approach, and the other two empirical approaches: APR1 and APR2.

The only firm-ish conclusion thus far, drawn only from the alfonsino analyses, is a preference for APR1 – maintain a slow steady increase in catch until the CPUE index might indicate a marked downward trend, rather than for APR2 - vary catches up and down in response to shorter-term CPUE changes. But even that is not very satisfactory, as certain control parameter value choices (especially the size of the initial upward trend in TACs) look likely to need to vary substantially from stock to stock, requiring stock-specific as well as generic analyses to proceed further.

At this juncture then, the prospects for developing entirely generic approaches/harvest strategies able to cover the major resources in the SIOFA region do not appear promising. A roadmap with suggestions about how SIOFA might best move forward towards adopting such harvest strategies in these circumstances will be put forward as the second part of this project.

REFERENCES

Brandão, A. Butterworth, D.S. and Johnston, S. 2020. Age-Structured Production Model (ASPM) assessments of the alfonsino (*Beryx splendens*) resource in the SIOFA area of the Southern Indian Ocean. 2nd Meeting of the Stock and Ecological Risk Assessment Working Group (SERAWG2). SERAWG2-02-14, 39pp.

Brouwer, S., Wrag, C., Wichman, M, and Nicholas, T. 2020. Alfonsino age and growth – rev1. In prep.

Cordue, P.L. 2018. Stock assessment of orange roughy in the Walter's Shoal Region. 1st Meeting of SIOFA Stock Assessment Working Group. SAWG(2018)-01-05 Rev1, 57pp.

Flores, A, Wiff, R, Galves, P and Diaz, E. 2012. Reproductive biology of alfonsino *Beryx spendens*. J. Fish. Biol. 1:1375-1390.

Ivanin, N and Rebyk, S. 2012. Age, growth parameters and some aspects of reproduction of alfonsino *Beryx splendens* Lowe on the Southwest Indian Ridge. YugNIRO, Ukraine. Working Paper. Workshop on Assessment and Management of alfonsino Fisheries. FAO, Rome, Italy, 10–12 January 2012. 4 pp.

Lehodey, R., Grandperrin, R. and Marchal, P. 1997. Reproductive biology and ecology of a deep-demersal fish, alfonsina, *Beryx spendens*, over the seamount off New Calendonia. Mar. Biol. 28:17-27.

Macaulay, G. 2021. Orange roughy acoustic data processing – estimation of the biomass. Final Report for Project SER2021-01, Terms of Reference 3.

Sarralde, R., Massiot-Granier, F., Selles, J. and Soeffker, M. 2020. Preliminary analysis of the Patagonian toothfish fishing data of the Del Cano Rise SIOFA. 2nd Meeting of the Stock and Ecological Risk Assessment Working Group (SERAWG2). SERAWG2-02-11, 32pp.

Table 1. Yearly catches of alfonsino (in tonnes) estimated to have been taken from the SIOFA area of the Southern Indian Ocean in the West area summed over fleets, and the standardised CPUE indices for "fleet" S2. Yearly catches of orange roughy and survey abundance indices (with CV) for Feature 4 are also listed.

Year	Alfonsino (West area)		Orange roughy (Feature 4)	
	Catches (tonnes)	CPUE (S2)	Catches (tonnes)	Survey (CV)
1977	—	—	—	—
1978	—	—	—	—
1979	—	—	—	—
1980	20	—	—	—
1981	2524	—	—	—
1982	921	—	—	—
1983	852	—	—	—
1984	57	—	—	—
1985	3	—	—	—
1986	—	—	—	—
1987	2	—	—	—
1988	16	—	—	—
1989	—	—	—	—
1990	—	—	—	—
1991	—	—	—	—
1992	314	—	—	—
1993	462	—	—	—
1994	1534	—	—	—
1995	2249	—	—	—
1996	3079	—	—	—
1997	1031	—	—	—
1998	859	—	—	—
1999	2111.9	—	—	—
2000	1979.2	—	—	—
2001	3587.3	2.088	144	—
2002	142.7	0.819	—	—
2003	357.2	—	—	—
2004	194.2	—	—	—
2005	434	—	203	—
2006	17.6	—	382	—
2007	98	—	650	7 923 (0.1)
2008	49.9	—	110	—
2009	3095	2.485	604	10 618 (0.3)
2010	3026.9	0.722	837	—
2011	3490.2	0.866	753	—
2012	4002.4	0.478	391	—
2013	4253.9	1.079	496	—
2014	2934.7	0.562	171	—
2015	4216.6	0.805	292	—
2016	3507.9	0.585	158	—
2017	4364.5	0.502	599	—
2018	2156.74	1.009	599††	6 500 (0.158)
2019	2156.74†	—	599††	—
2020	2156.74†	—	599††	—
2021 (TAC)	2160†		600††	

† Catches assumed to be equal to those in 2018.

†† Catches assumed to be equal to those in 2017.

Table 2. Biological parameter and ASPM parameter values assumed/estimated for the Base case Operating Model for alfonsino and for orange roughy. Note that for simplicity, maturity is assumed to be knife-edged in age.

Biological Parameter	Alfonsino	Orange roughy
Natural mortality M (yr^{-1})[1]	0.2	0.045
von Bertalanffy growth[2]		
ℓ_∞ (cm)	69.21	46.75
κ (yr^{-1})	0.05	0.069
t_0 (yr)	-6.12	-0.5
Weight (in kg) length (in cm) relationship[3]		
c	2.9×10^{-5}	2.65×10^{-4}
d	2.98	2.436
Age at maturity (yr) a_m[4]	6	37
Steepness parameter (h)	0.75	0.75
ASPM parameter estimates		
Selectivity parameters		
a_{50} (yr)	14.15	Knife edge at age 37
δ (yr^{-1})	1.968	
Spawning biomass K^{sp} (tonnes)	49 138	11 593
MSY (tonnes)	3 325	271
CPUE/Survey parameters		
σ_{CPUE}	0.465	0.17†
q_{CPUE}	$9.90\text{x}10^{-05}$	$\sim\text{LN}(0.8, 0.19^2)$

† Approximately the average of the observed historical CVs.

[1] Taken from TOR document.
[2] Brouwer (2002)
[3] Ivanin and Rebyk (2012)
[4] Lehodey *et al*. (1997); Flores *et al*. (2012)

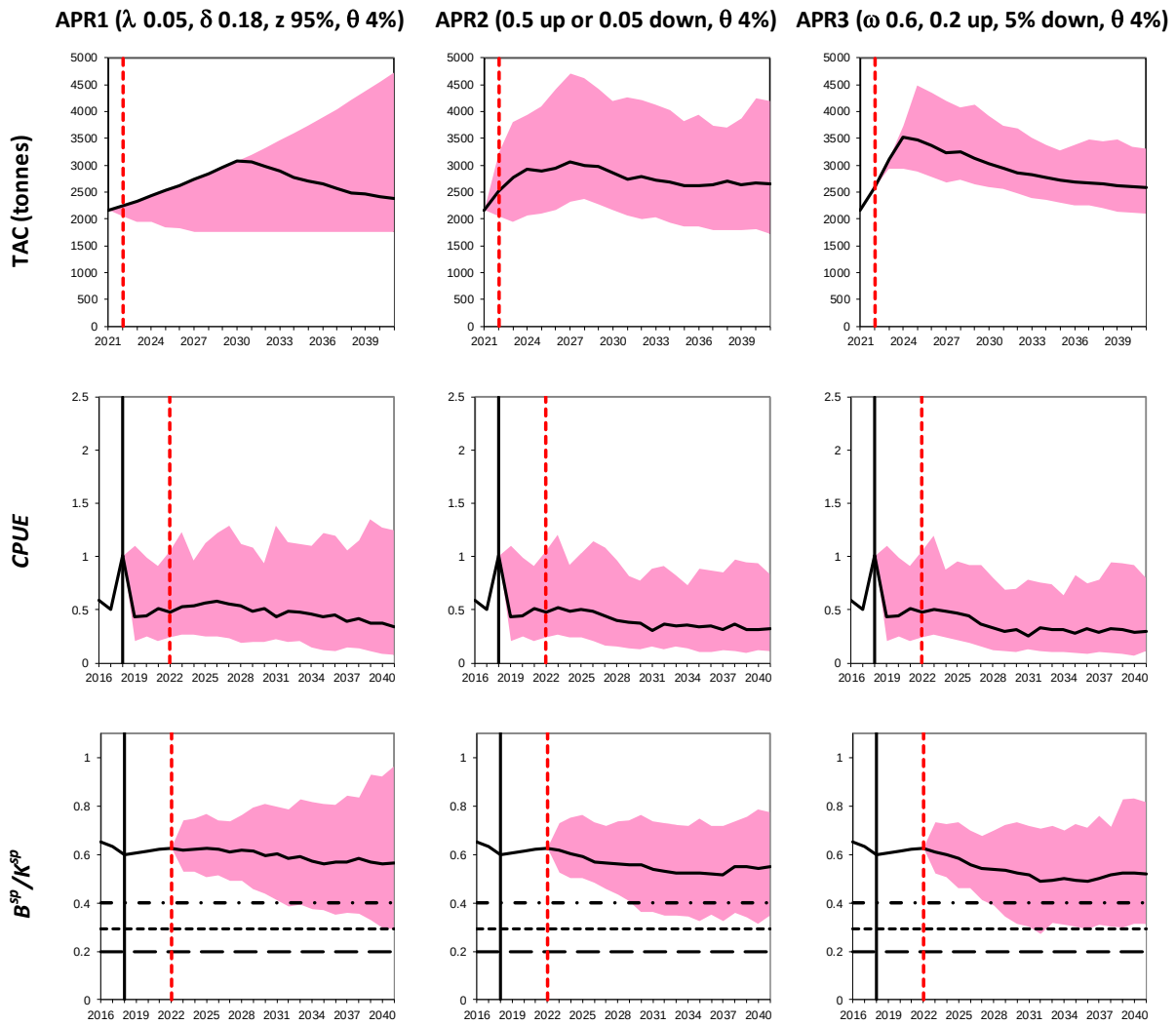

Figure 1. Comparison of summary median trajectories for APR1 (left), APR2 (middle) and APR3 (right) for **alfonsino** in the West area. Results are shown for one option of each of the APRs. The dashed lines for the depletion plots (middle plot) are in order from the bottom: Limit Reference Point (RP), B_{MSY}/K and Target RP. The shaded areas represent 90% probability envelopes.

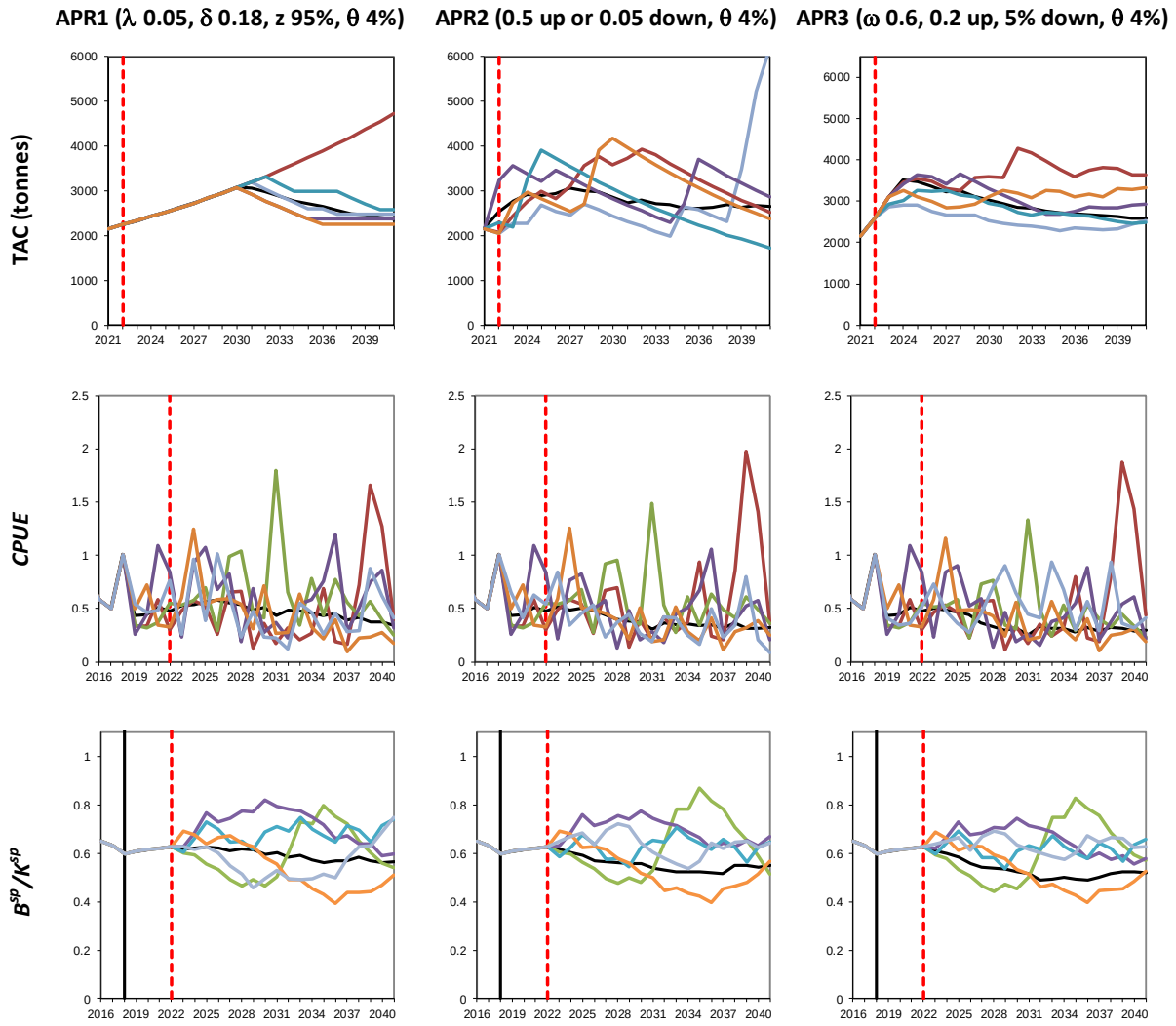

Figure 2. Median trajectories (thick black lines) of the TAC (in tonnes), CPUE trends and spawning biomass depletion for one option of each of APR1 (left), APR2 (middle) and APR (right) for **alfonsino** in the West area. Projections commence to the right of the thick black vertical lines but with observed data (in the case of catches) until the red dashed vertical lines. A random selection of worm plots is also shown (coloured lines).

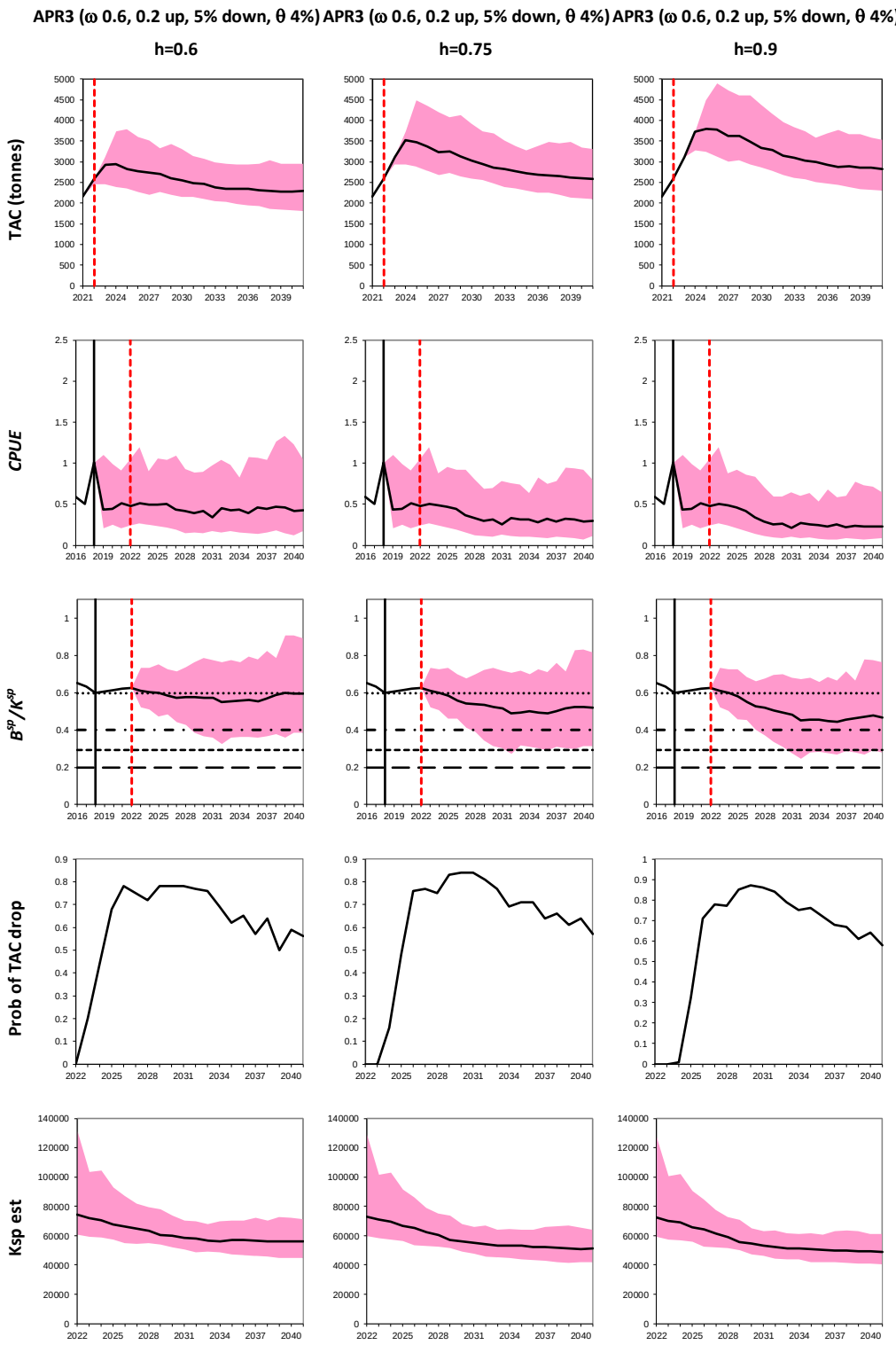

Figure 3. Summary median trajectories for **APR3 for alfonsino** assuming different values for the steepness parameter h in the assessment model to set a TAC. The dashed lines for the depletion plots (middle plot) are in order from the bottom: Limit RP, B_{MSY}/K and Target RP. The shaded areas represent 90% probability envelopes.

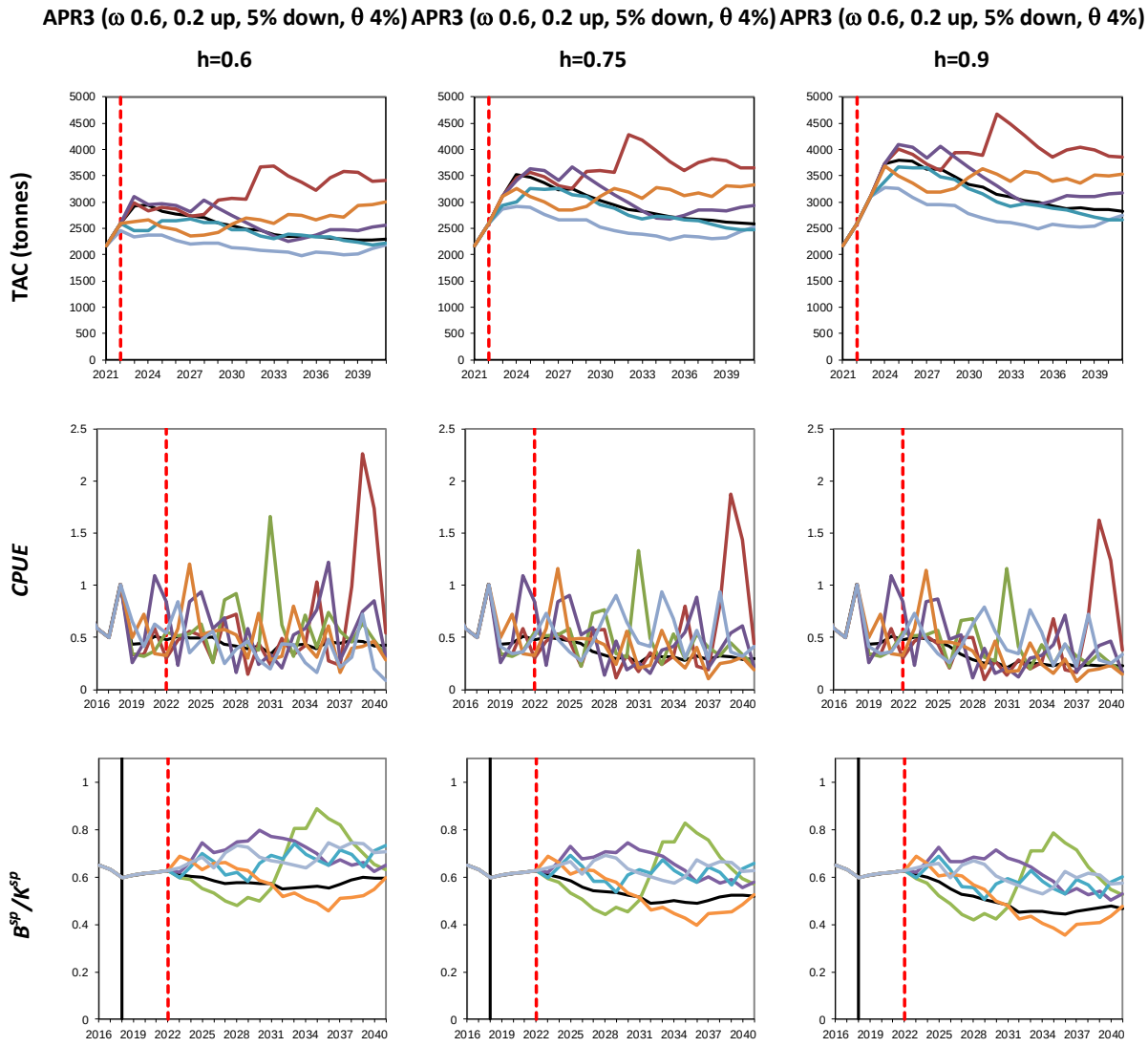

Figure 4. Summary median trajectories for **APR3 for alfonsino** assuming different values for the steepness parameter h in the assessment model to set a TAC. Projections commence to the right of the thick black vertical lines but with observed data (in the case of catches) until the red dashed vertical lines. A random selection of worm plots is also shown (coloured lines).

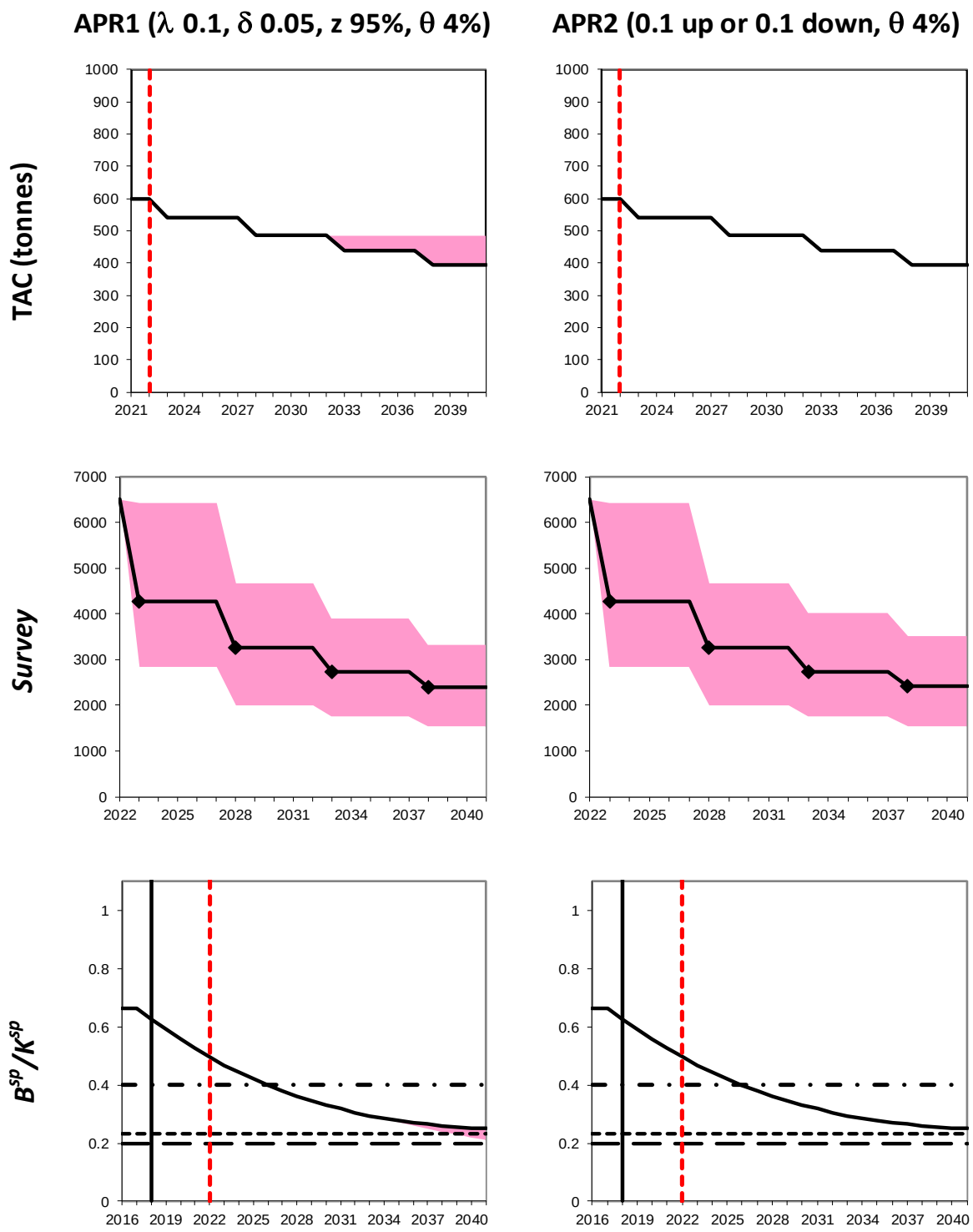

Figure 5. Comparison of summary median trajectories for APR1 (left) and APR2 (right) for orange roughy in Feature 4. Results are shown for one option of each of the APRs. The dashed lines for the depletion plots (middle plot) are in order from the bottom: Limit RP, B_{MSY}/K and Target RP. The shaded areas represent 90% probability envelopes.

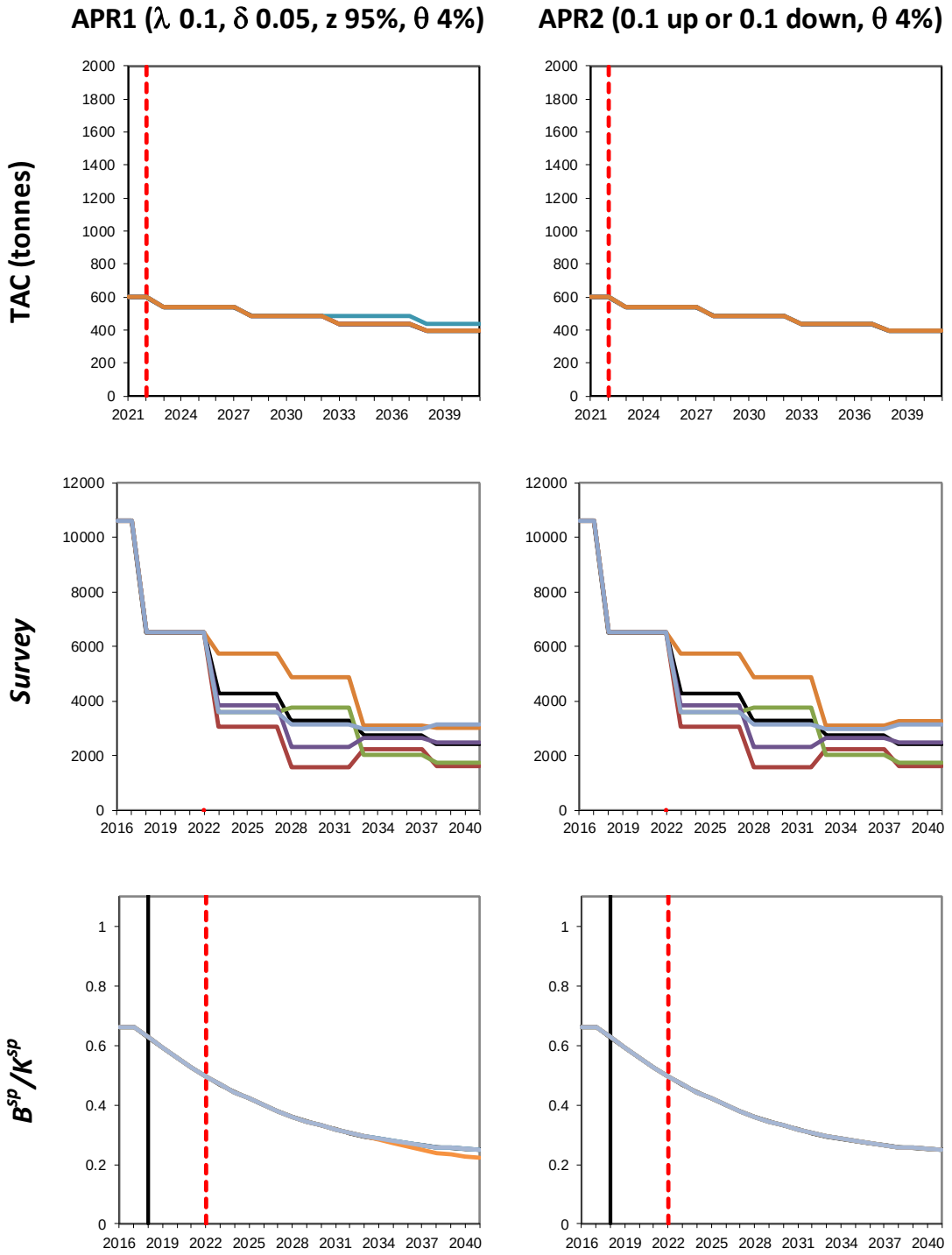

Figure 6. Median trajectories (thick black lines) of the TAC (in tonnes), CPUE trends and spawning biomass depletion for one option of each of APR1 (left) and APR2 (right) for **orange roughy** in Feature 4. Projections commence to the right of the thick black vertical lines but with observed data (in the case of catches) until the red dashed vertical lines. A random selection of worm plots is also shown (coloured lines).

Appendix A

Generation of future data

Alfonsino

The approaches investigated for alfonsino assume that commercial CPUE data will continue to be available annually in the future.

The evaluation of the approaches being investigated requires the simulation of such future CPUE data from projections for the population. These projections are carried out using the following procedure.

1. Numbers-at-age ($N_{y',a}$) for the start of the year in which projections commence (i.e. *y'* = 2022) are calculated by applying equations (A1.1)–(A1.3) given below. To allow for initial variation in biomass projections (as the stochastic effects enter later only through variability in future recruitment which takes a period to propagate through to the exploitable component of the biomass), the numbers-at-age for the first seven years are allowed to vary, where these variations are simulated by generating $\varphi_{y'}$ factors distributed as $N(0, \sigma_R^2)$, where $\sigma_R = 0.5$. Thus, for ages 1–7, the numbers-at-age are given by $N_{y',a} e^{\left(\varphi_{y'} - \frac{\sigma_R^2}{2}\right)}$. The future catches-at-age ($C_{y',a}$) are obtained from equations (A1.4) and (A1.5). Such future catch-at-age values are generated under the assumption that the commercial selectivity function remains the same as that for the last year of the assessment. Future recruitments are obtained from the stock-recruitment relationship given by equation (A1.8), which allows for fluctuations about this relationship. These fluctuations are computed for each future year simulated by generating $\zeta_{y'}$ factors distributed as $N(0, \sigma_R^2)$, where $\sigma_R = 0.5$.

2. Future spawning and exploitable biomasses are calculated using equations (A1.6) and (A1.7). Given the exploitable biomass, the expected CPUE abundance index $I_{y'}^{CPUE}$ is first generated using equation (A1.9); then a log-normally distributed observation error is added to this expected value. Hence projections of the CPUE are given by:

$$I_{y'}^{CPUE} = q_{CPUE} B_{y'}^{\exp} e^{\varepsilon_{y'}},$$

   where $\varepsilon_{y'}$ is normally distributed with a mean zero and a standard deviation σ_{CPUE} whose value is given by the estimate obtained for the operating model (equation (A1.11)) as is q_{CPUE} (from equation (A1.10)), for the fishery.

3. The true catch ($C_{y'}$) (removal from the population) is given by the set $TAC_{y'}$

   The numbers-at-age for year *y'* are projected forward under this true catch (removal); the operating model is used to obtain values for $C_{y',a}$ and $N_{y'+1,a}$. The same assumptions about the commercial selectivity function and recruitment fluctuations as made in step (1) above are also made for these projections.

4. Steps (2)–(3) are repeated for each future year considered.

5. This projection procedure is replicated 100 times, to provide the probability distributions for projection results arising from uncertainties in future recruitment and observation errors in CPUE (which in turn affect future catches and consequently numbers in the population and the number of recaptures).

The Alfonsino population dynamics are described by the equations

$$N_{y+1,0} = R(B^{sp}_{y+1}) \tag{A1.1}$$

$$N_{y+1,a+1} = (N_{y,a} - C_{y,a})\ e^{-M} \qquad 0 \leq a \leq m\text{-}2 \tag{A1.2}$$

$$N_{y+1,m} = (N_{y,m} - C_{y,m})\ e^{-M} + (N_{y,m-1} - C_{y,m-1})\ e^{-M} \tag{A1.3}$$

where

$N_{y,a}$ is the number of alfonsino of age a at the start of year *y*,

$C_{y,a}$ is the number of alfonsino of age a taken by the fleets in year *y*,

$R(B^{sp})$ is the Beverton-Holt stock-recruitment relationship,

B^{sp} is the spawning biomass at the start of year *y*,

M is the natural mortality rate of alfonsino (assumed to be independent of age), and

m is the maximum age considered (i.e. the "plus group").

Note that in the interests of simplicity, this approximates the fishery as a pulse fishery at the start of the year. Given that alfonsino are relatively long-lived with low natural mortality, such an approximation would seem adequate.

For a fishery for which CPUE series are available for three different fleets, the total predicted number of fish of age *a* caught in year *y* is given by

$$C_{y,a} = \sum_{f=1}^{3} C^{f}_{y,a}, \tag{A1.4}$$

where

$$C^{f}_{y,a} = N_{y,a} S^{f}_{y,a} F^{f}_{y} \tag{A1.5}$$

and

F^{f}_{y} is the proportion of the resource above age *a* harvested in year *y* by fleet *f*, and

$S^{f}_{y,a}$ is the commercial selectivity at age a in year *y* for fleet *f*, described by a logistic curve.

The spawning biomass in year *y* is given by

$$B^{sp}_{y} = \sum_{a=1}^{m} w_a f_a\, N_{y,a} = \sum_{a=a_m}^{m} w_a\, N_{y,a} \tag{A1.6}$$

where

f_a is the proportion of fish of age *a* that are mature (assumed to be knife-edge at age a_m), and

w_a is the mass of a fish at age *a*.

The model estimate of the fleet-specific exploitable component of the biomass is given by

$$B_y^{\exp}(f) = \sum_{a=0}^{m} w_a S_{y,a}^f N_{y,a}\,.$$

(A1.7)

The number of recruits at the start of year *y* is assumed to be related to the spawning biomass at the start of year *y*, B_y^{sp}, by a Beverton-Holt stock-recruitment relationship. To allow for stochastic recruitment, this is given by

$$R\left(B_y^{sp}\right) = \frac{\alpha B_y^{sp}}{\beta + B_y^{sp}} e^{\left(\zeta_y - \sigma_R^2/2\right)}, \qquad \text{(A1.8)}$$

where ζ_y reflects fluctuation about the expected recruitment for year *y*, which is assumed to be normally distributed with standard deviation σ_R (which is input). The values of the parameters α and β can be calculated given the unexploited equilibrium (pristine) spawning biomass K^{sp} and the steepness of the curve *h*.

The observed (standardised) CPUE abundance indices are assumed to be lognormally distributed about their expected values

$$I_y^f = \hat{I}_y^f e^{\varepsilon_y^f} \text{ or } \varepsilon_y^f = ln\left(I_y^f\right) - ln\left(\hat{I}_y^f\right), \qquad \text{(A1.9)}$$

where

I_y^f is the standardised CPUE series index for year *y* corresponding to fleet *f*,

$\hat{I}_y^f = \hat{q}^f \hat{B}_y^{\exp}(f)$ is the corresponding model estimate, where

$\hat{B}_y^{\exp}(f)$ is the model estimate of exploitable biomass of the resource for year *y* corresponding to fleet *f*, and

$\hat{q}^f$ is the catchability coefficient for the standardised commercial CPUE abundance indices for fleet *f*, whose maximum likelihood estimate is given by

$$\widehat{ln\, q^f} = \frac{1}{n^f}\sum_y \left(ln\, I_y^f - \widehat{ln\, B_y^{\exp}}\,(f)\right), \qquad \text{(A1.10)}$$

where

n^f is the number of data points in the standardised CPUE abundance series for fleet *f*, and

ε_y^f is normally distributed with mean zero and standard deviation σ^f (assuming homoscedasticity of residuals), whose maximum likelihood estimate is given by

$$\hat{\sigma}^f = \sqrt{\frac{1}{n^f}\sum_y \left(ln\, I_y^f - \widehat{ln\, q^f}\, \hat{B}_y^{\exp}(f)\right)^2}. \qquad \text{(A1.11)}$$

Orange roughy

The approaches investigated for orange roughy assume that new acoustic survey estimates of abundance will continue to become available every five years in the future.

The methodology to generate future data for orange roughy is basically the same as given above for alfonsino, except for point 2 there. Given the exploitable biomass, the expected acoustic survey abundance index $I_{y'}^{Survey}$ is first generated using equation (A1.9); then a log-normally distributed random sampling error is added to this expected value. A systematic error that accounts for the uncertainty about the absolute value is then also added, and is assumed to remain unchanged over time within in a particular simulation realisation of a trajectory. Hence projections of the acoustic surveys are given by

$$I_{y'}^{Survey} = q_{Survey} B_{y'}^{\exp} e^{\xi + \varepsilon_{y'}^{Survey}}$$

where $\varepsilon_{y'}^{Survey}$ is normally distributed with a mean zero and a standard deviation σ_{Survey}, whose value is given by the approximate average of the historical sampling CVs, and e^{ξ} is normally distributed with a mean of 0.8 and standard deviation of 0.19 (the prior distribution assumed by Cordue (2018)).

Appendix B

Results for Alfonsino in the West area of the SIOFA region

Results for different choices for the values for the control parameter for APR1, APR2 and APR3 are shown below. Initial investigation of APR1 led to the selection of control parameters of $\delta = 0.18$, the lower bound of a 95th confidence interval ($\alpha = 0.05$), and $\lambda = 0.05$. Results shown are for different values of the control parameter θ (2%, 3% and 4%) (Figures B.1 and B.2).

Various values (20% and 50%) of the maximum inter-annual increase change in TAC allowed, and for a value of 5% for the maximum decrease change in TAC for APR2 (Figures B.3 and B.4).

Figures B.5 and B.6 show results for APR3 for different values of the control parameter ω.

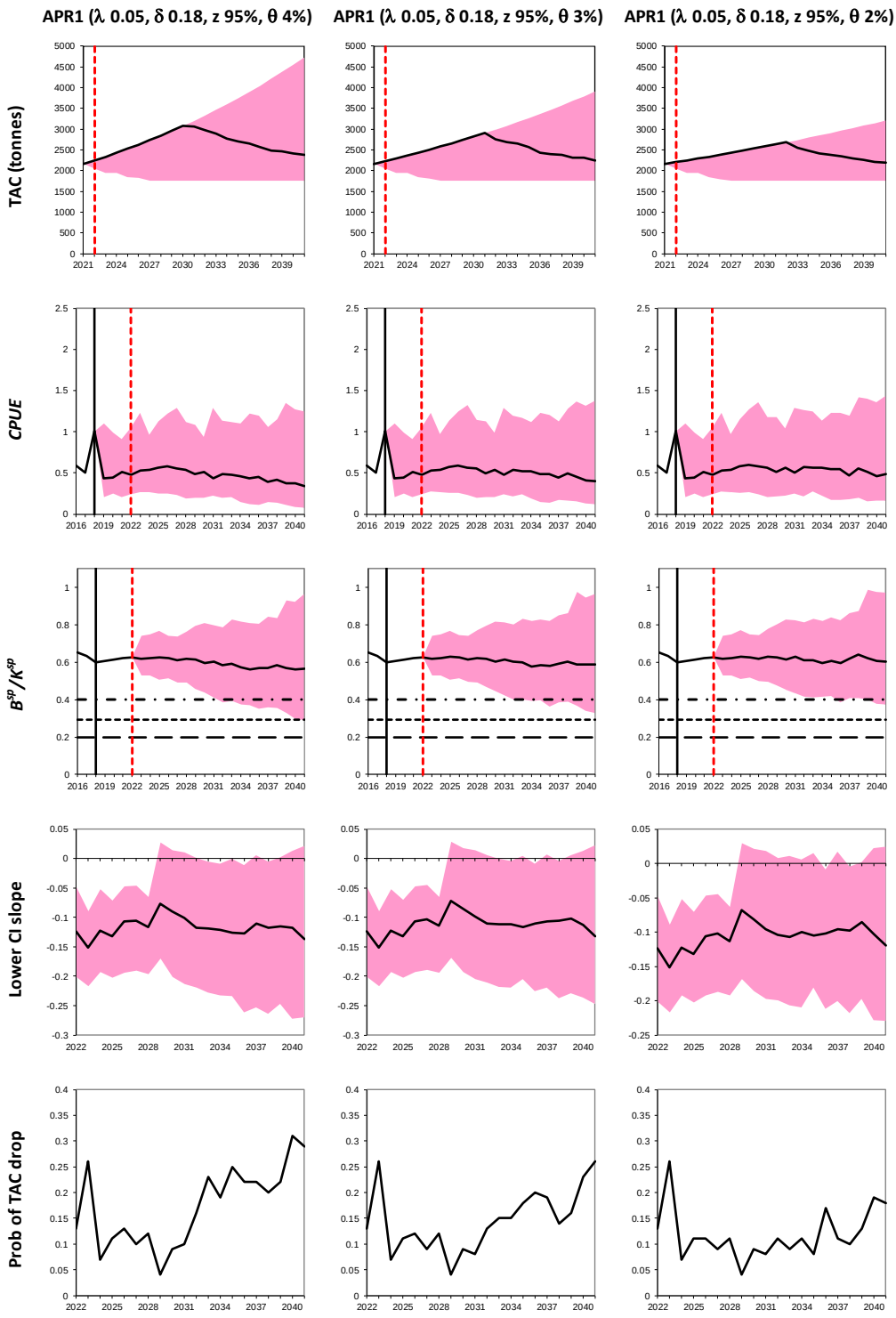

Figure B.1. Summary median trajectories for **APR1**. Results are shown for different values of θ (the initial amount the TAC is increased until the first TAC decrease), while the λ values are fixed at 0.05 (amount by which the TAC is decreased), the δ values are fixed at 0.18 (the value of the downward trend beyond which the TAC will be modified) and the lower confidence limit of the slope is for a 95% CI. The dashed lines for the depletion plots (middle plot) are in order from the bottom: Limit RP, B_{MSY}/K and Target RP. The shaded areas represent 90% probability envelopes.

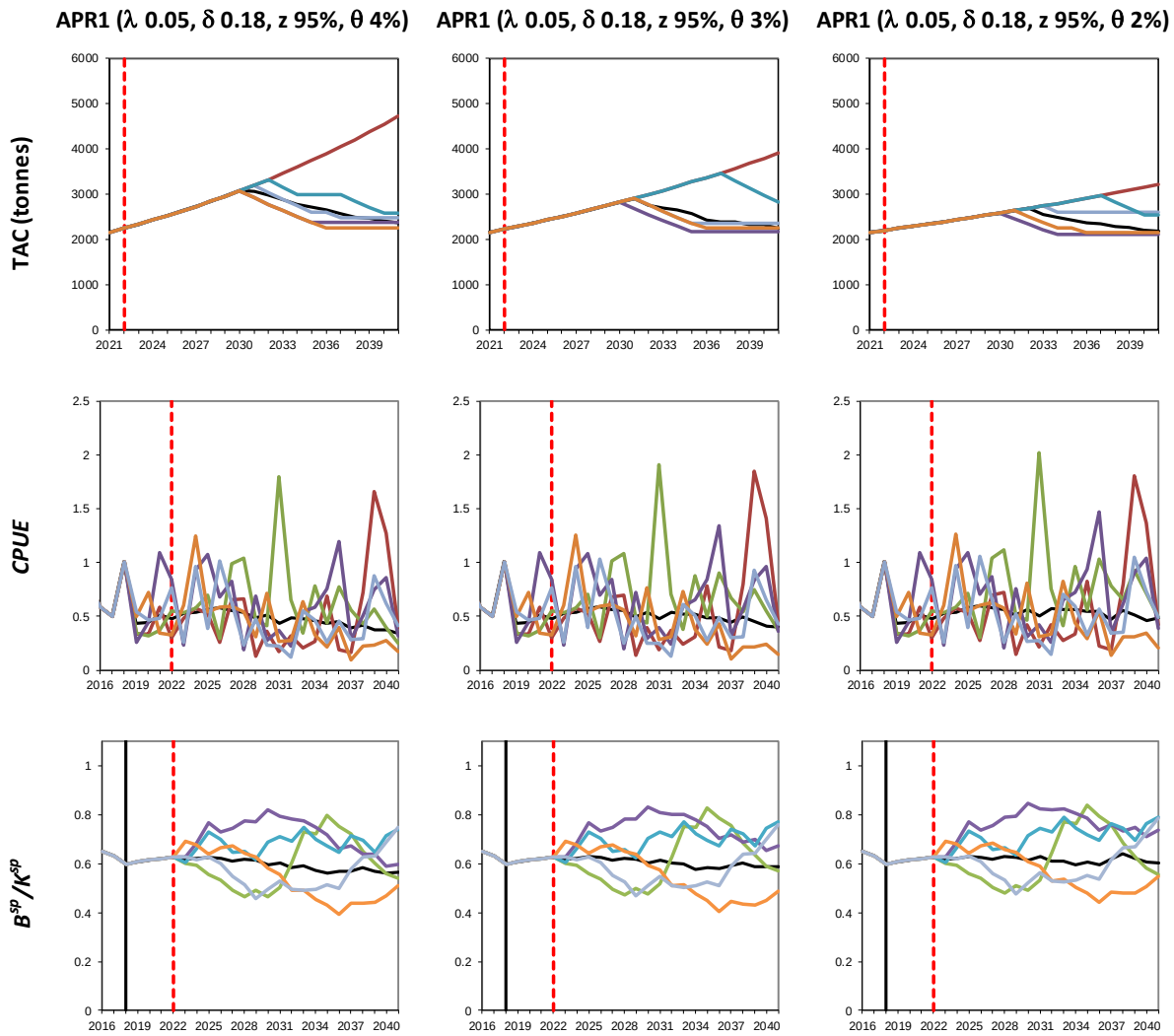

Figure B.2. Median trajectories (thick black lines) of the TAC (in tonnes), CPUE trends and spawning biomass depletion for for different values of θ (the initial amount the TAC is increased until the first TAC decrease) for **APR1**. Projections commence to the right of the thick black vertical lines but with observed data (in the case of catches) until the red dashed vertical lines. A random selection of worm plots is also shown (coloured lines).

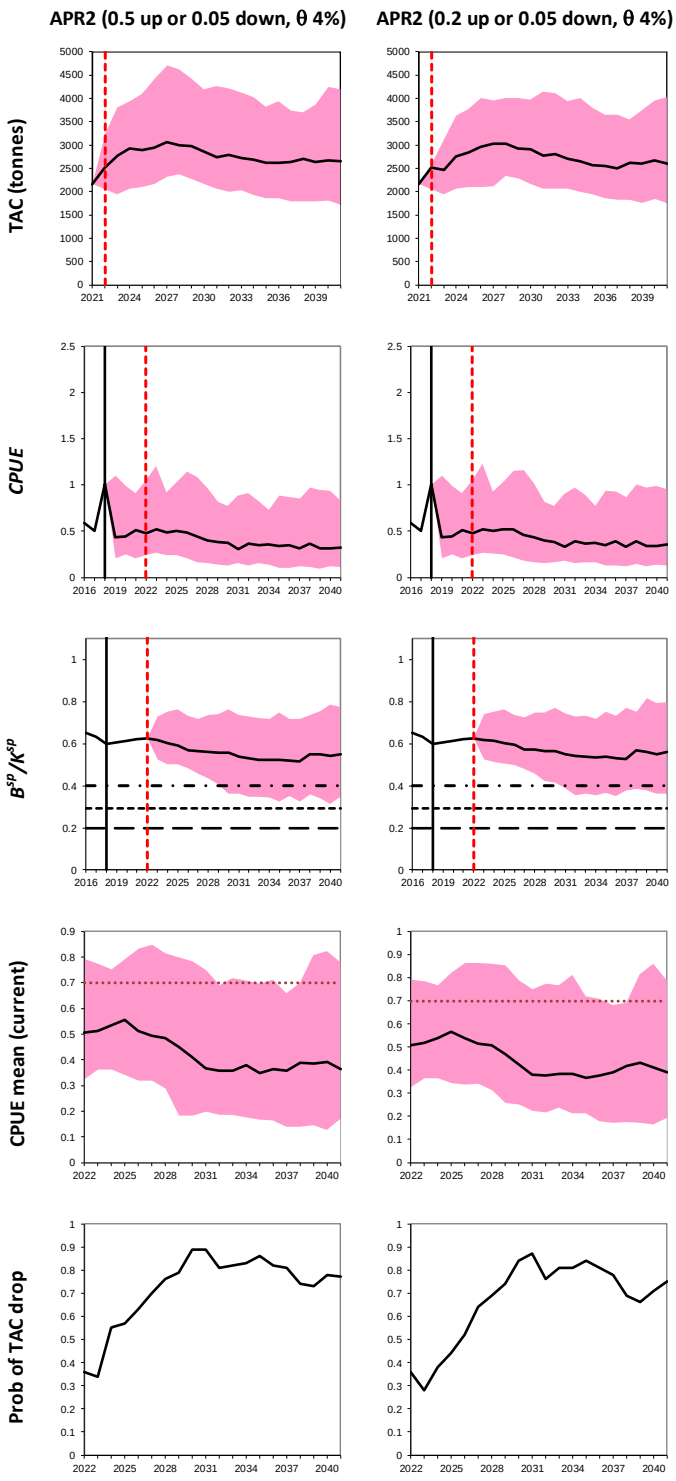

Figure B.3. Summary median trajectories for **APR2**. Results are shown for a fixed value of θ (the initial amount the TAC is increased until the first TAC decrease) and for different values for the constraint on the inter annual increase change in TAC, while the constraint on the inter annual decrease change is fixed at 5%. The dashed lines for the depletion plots (middle plot) are in order from the bottom: Limit RP, B_{MSY}/K and Target RP. The shaded areas represent 90% probability envelopes.

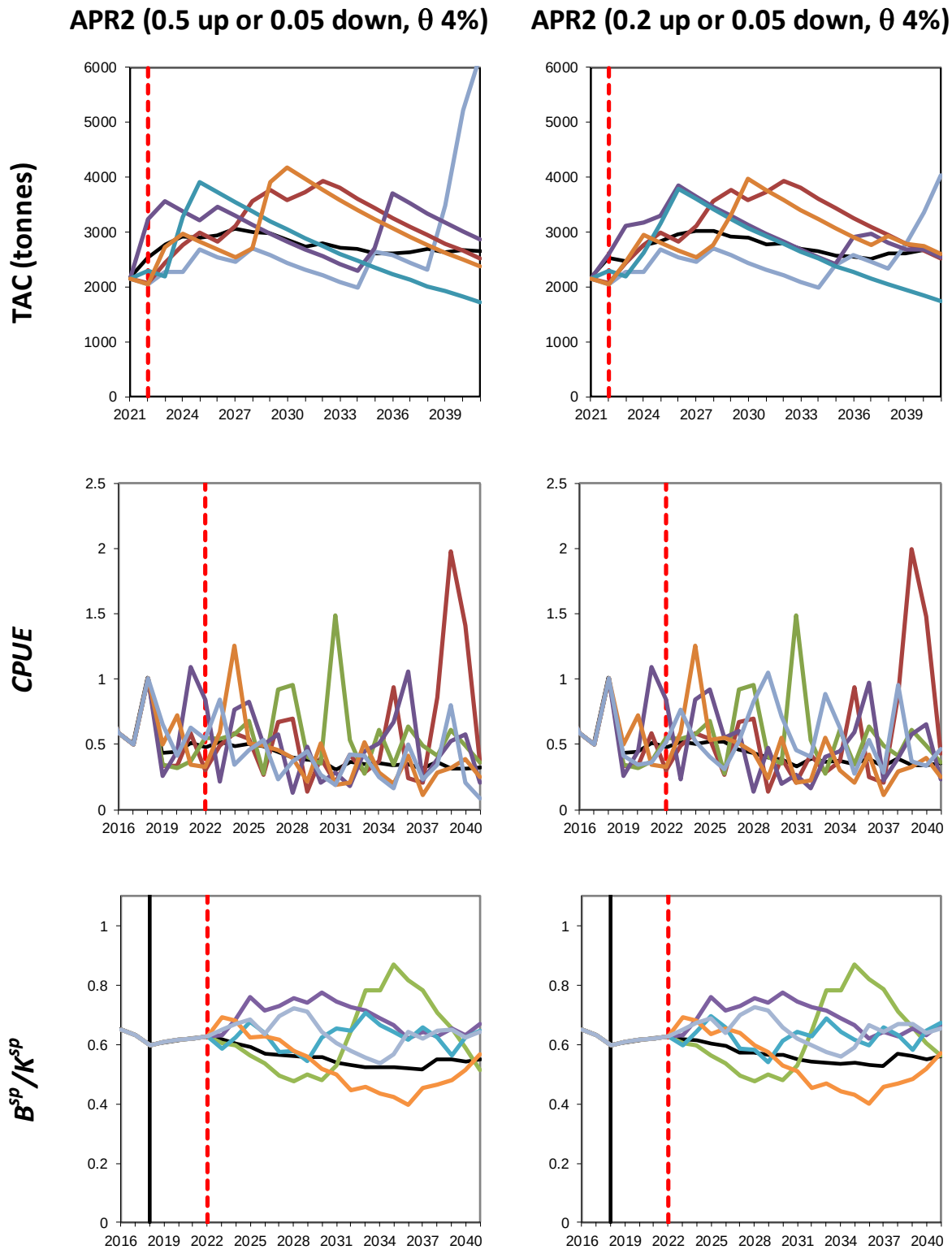

Figure B.4. Median trajectories (thick black lines) of the TAC (in tonnes), CPUE trends and spawning biomass depletion for different values for the constraint on the inter annual increase change in TAC for **APR2**. Projections commence to the right of the thick black vertical lines but with observed data (in the case of catches) until the red dashed vertical lines. A random selection of worm plots is also shown (coloured lines).

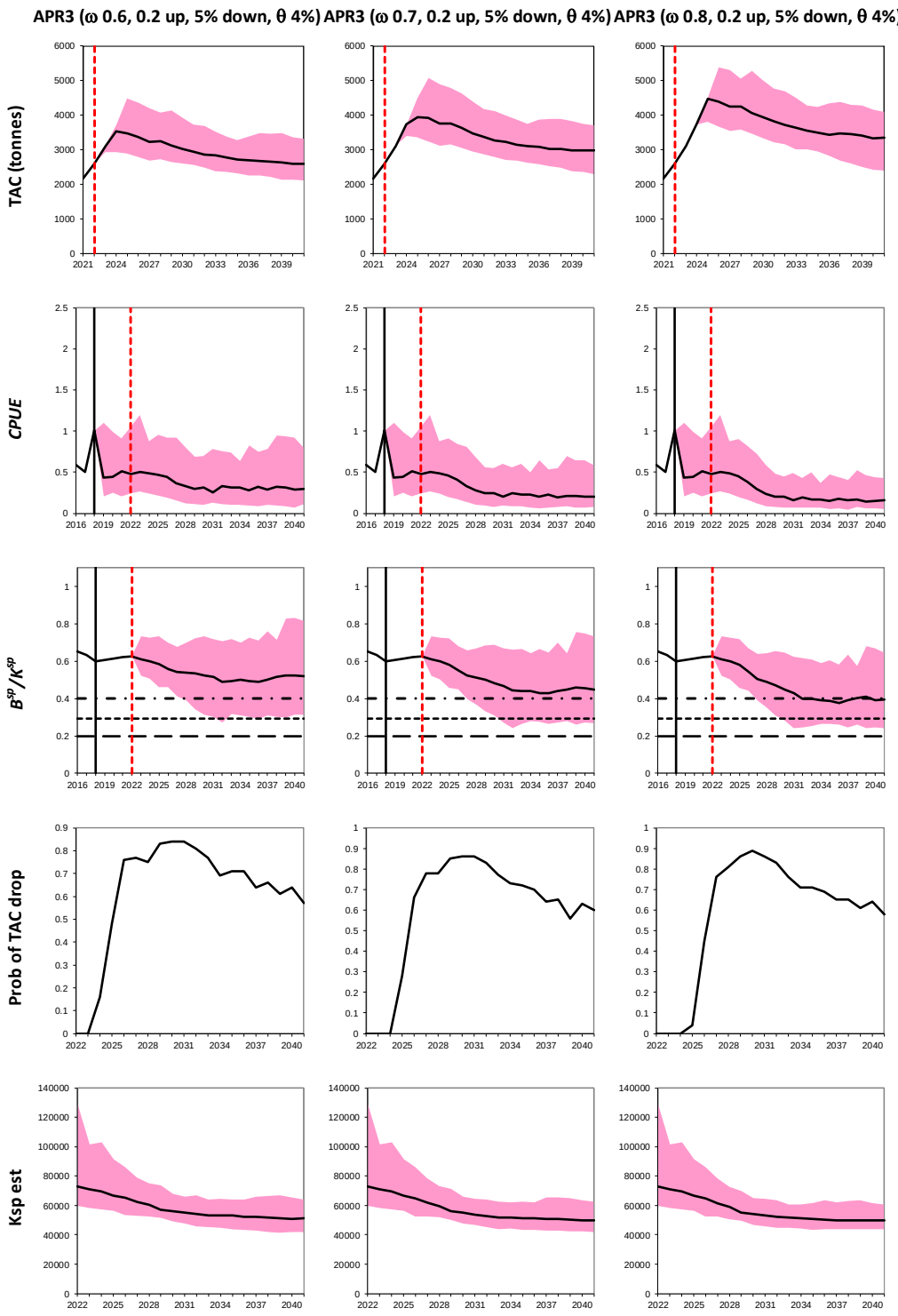

Figure B.5. Summary median trajectories for **APR3**. Results are shown for different values of the control parameter ω and a fixed values of θ (the initial amount the TAC is increased until the first TAC decrease) and the constraint on the inter annual change in TAC. The dashed lines for the depletion plots (middle plot) are in order from the bottom: Limit RP, B_{MSY}/K and Target RP. The shaded areas represent 90% probability envelopes.

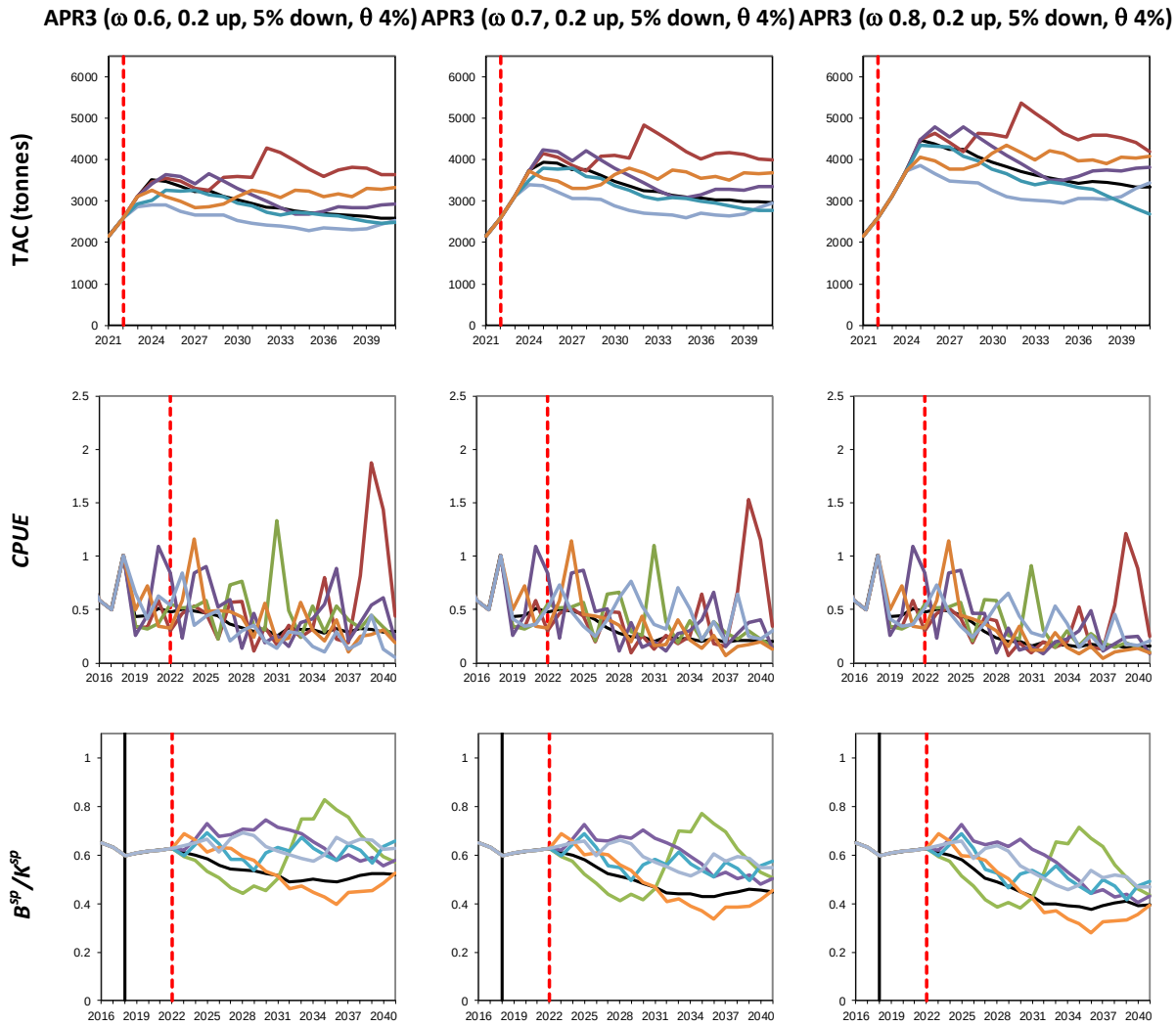

Figure B.6. Median trajectories (thick black lines) of the TAC (in tonnes), CPUE trends and spawning biomass depletion for different values of the control parameter ω for **APR3**. Projections commence to the right of the thick black vertical lines but with observed data (in the case of catches) until the red dashed vertical lines. A random selection of worm plots is also shown (coloured lines).

Appendix C

Results for Orange roughy for Feature 4 of the SIOFA region

Results for different choices for the values for the control parameter for APR1 and APR2 are shown below. Initial investigation of APR1 led to the selection of control parameters of $\delta = 0.05$, the lower bound of a 95th confidence interval ($\alpha = 0.05$), and $\theta = 0.04$. Results shown are for different values of the control parameter λ (0.1 and 0.15) (Figures C.1 and C.2).

Results are shown for various values (10% and 50%) of the maximum inter-annual increase or decrease change in TAC allowed. (Figures C.3 and C.4).

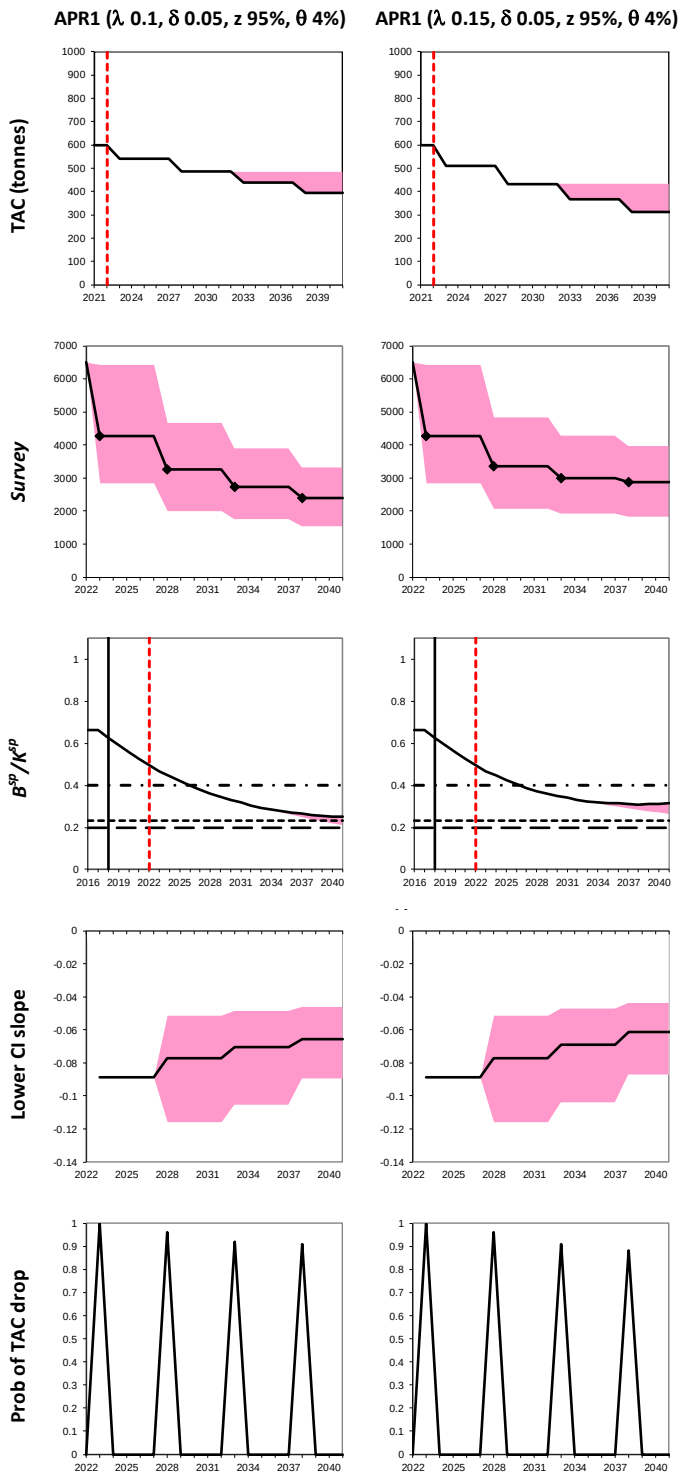

Figure C.1. Summary median trajectories for **APR1**. Results are shown for different values of λ (amount by which the TAC is decreased) and δ (the value of the downward trend beyond which the TAC will be modified), while values of θ (the initial amount the TAC is increased until the first TAC decrease) and the lower confidence limit of the slope are fixed. The dashed lines for the depletion plots (middle plot) are in order from the bottom: Limit RP, B_{MSY}/K and Target RP. The shaded areas represent 90% probability envelopes.

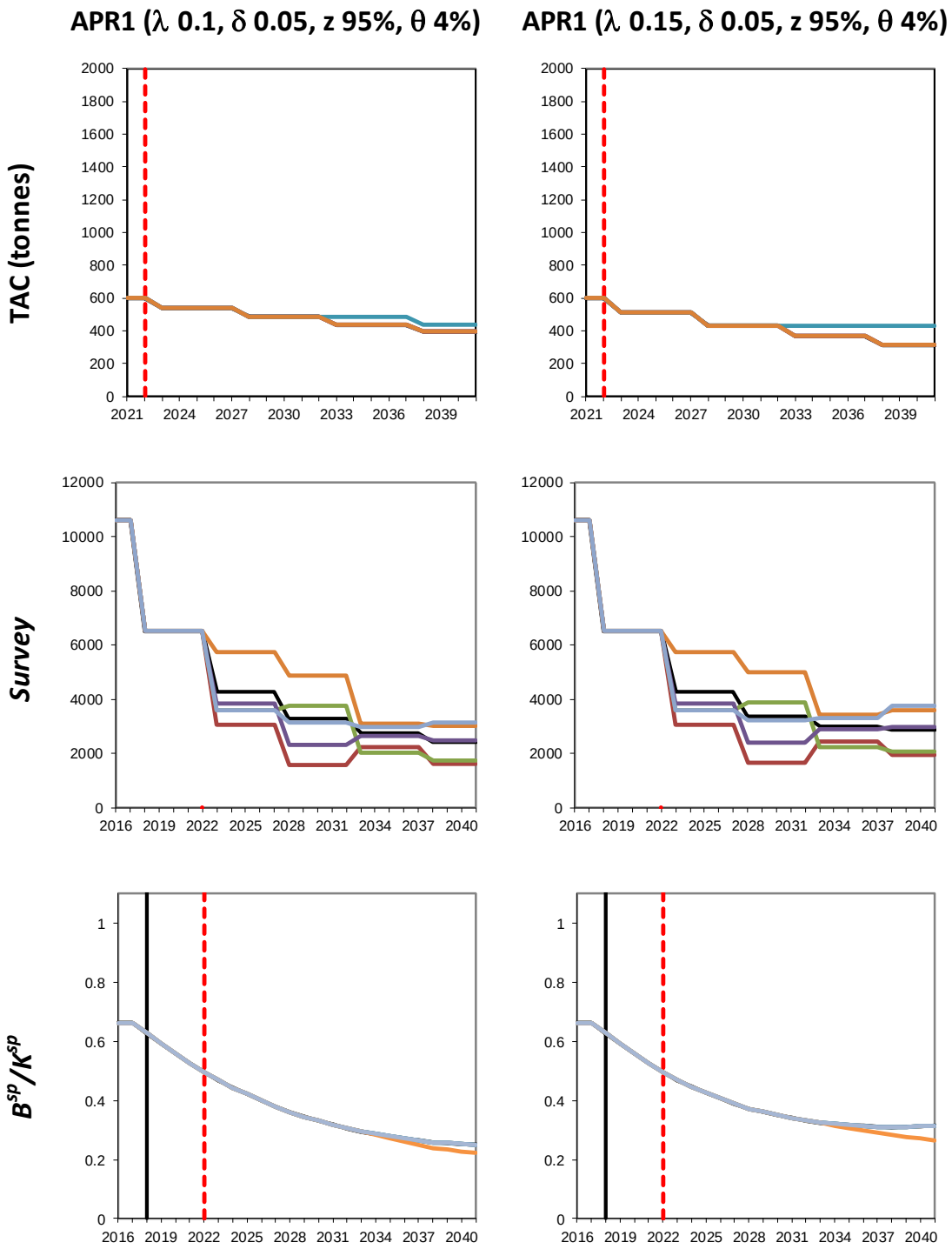

Figure C.2. Median trajectories (thick black lines) of the TAC (in tonnes), CPUE trends and spawning biomass depletion for different values of λ (amount by which the TAC is decreased) and δ (the value of the downward trend beyond which the TAC will be modified) for **APR1**. Projections commence to the right of the thick black vertical lines but with observed data (in the case of catches) until the red dashed vertical lines. A random selection of worm plots is also shown (coloured lines).

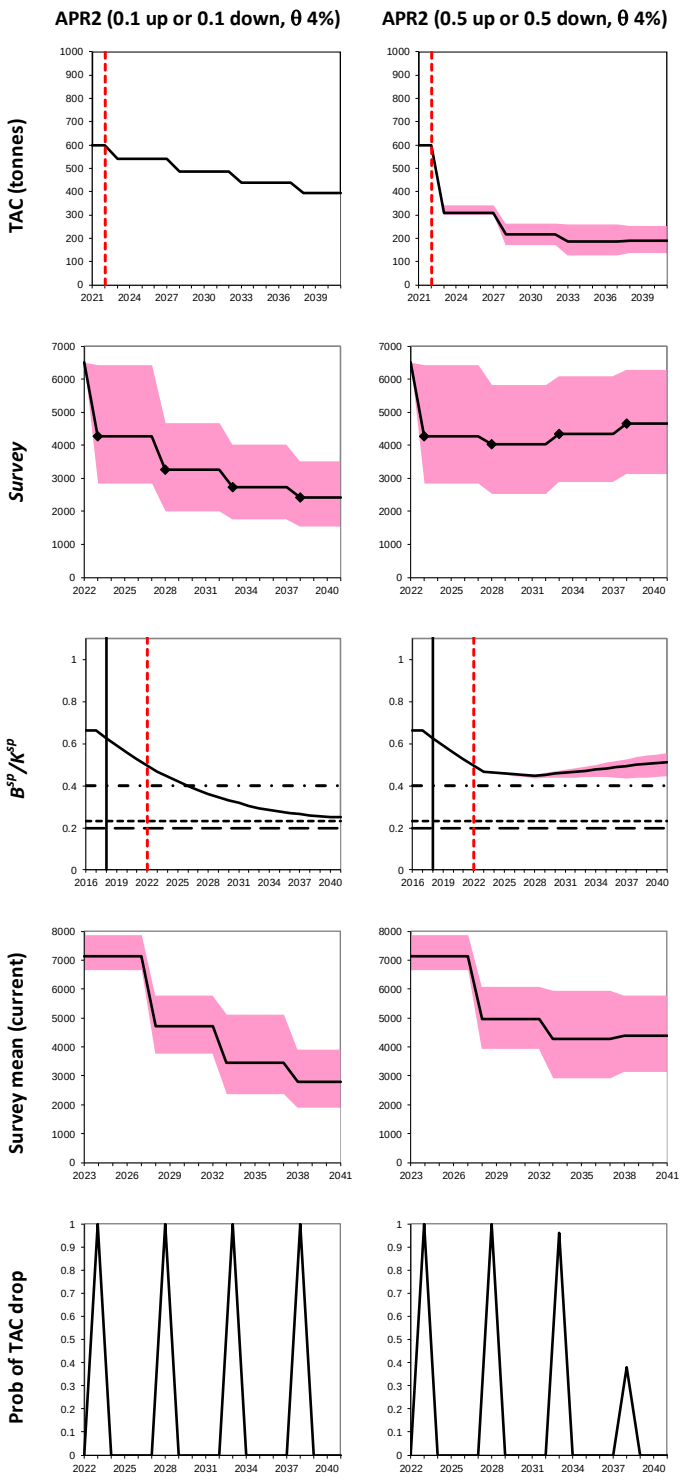

Figure C.3. Summary median trajectories for **APR2**. Results are shown for a fixed value of θ (the initial amount the TAC is increased until the first TAC decrease) and for different values for the constraint on the inter annual change in TAC. The dashed lines for the depletion plots (middle plot) are in order from the bottom: Limit RP, B_{MSY}/K and Target RP. The shaded areas represent 90% probability envelopes.

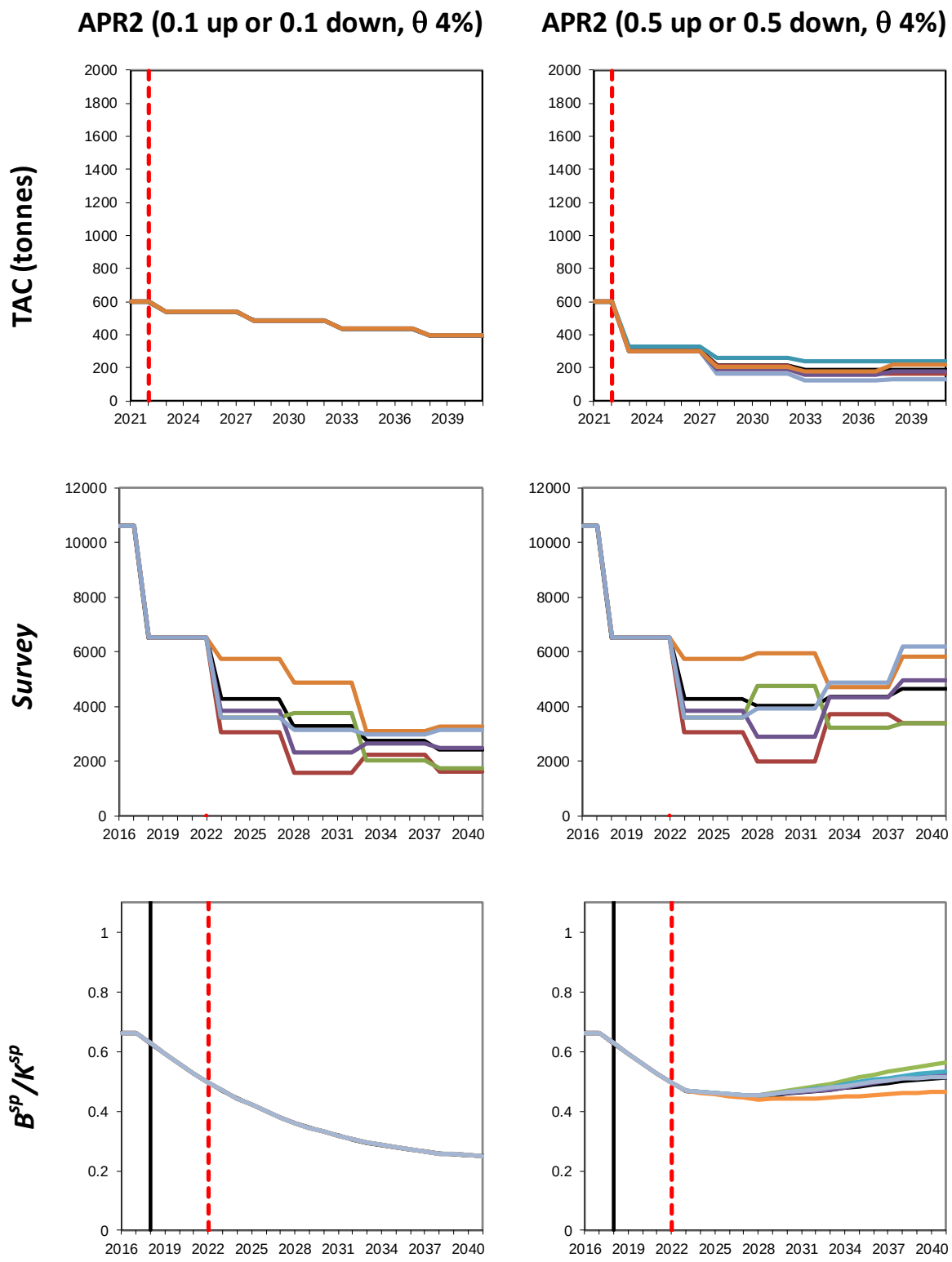

Figure C.4. Median trajectories (thick black lines) of the TAC (in tonnes), CPUE trends and spawning biomass depletion for different values for the constraint on the inter annual change in TAC for **APR2**. Projections commence to the right of the thick black vertical lines but with observed data (in the case of catches) until the red dashed vertical lines. A random selection of worm plots is also shown (coloured lines).